

High-temperature magnetic stability of small magnetite particles

Adrian R. Muxworthy¹ and David J. Dunlop

Geophysics, Department of Physics, University of Toronto, Toronto, Canada

Wyn Williams

School of GeoSciences, University of Edinburgh, Edinburgh, UK

Received 9 September 2002; revised 24 January 2003; accepted 28 February 2003; published 30 May 2003.

[1] The stability of magnetic domain structures of small grains of magnetite were examined between room temperature and the Curie temperature using a high-resolution three-dimensional micromagnetic algorithm. At all times the minimum resolution used was determined by calculating the exchange length. Using an unconstrained model, the single domain (SD) to multidomain (MD) threshold grain size d_0 was found to be nearly independent of temperature up to $\sim 450^\circ\text{C}$. Above this temperature, d_0 was observed to rise sharply. Energy barriers between metastable domain states trapped in local energy minimums (LEM) were determined using a constrained algorithm. Three types of domain structure were considered: SD, vortex, and double vortex (effectively three domain), in a range of grain sizes with side length between 30 and 300 nm. In addition, the effect of varying shape was also considered by examining asymmetric grains with aspect ratios up to 1.4. From the numerical solutions energy barriers between LEM states were determined. It was found that MD grains 300 nm in size display higher stability than smaller SD grains (~ 50 nm). Double vortex states were found to be less stable than single vortex states at nearly all temperatures. Blocking temperatures as function of grain size for both symmetric and asymmetric grains were determined and agree well with experimental results. Transdomain thermoremanence analysis indicated that there are a limited number of grain sizes and shapes which will nucleate domain wall-type structures during cooling. Such nucleation events would cause the total measured remanence to decrease with cooling in conflict with Néel's analytical theory for remanence cooling behavior but in agreement with experimental observations. *INDEX TERMS*: 1521 Geomagnetism and Paleomagnetism: Paleointensity; 1533 Geomagnetism and Paleomagnetism: Remagnetization; 1540 Geomagnetism and Paleomagnetism: Rock and mineral magnetism; 1599 Geomagnetism and Paleomagnetism: General or miscellaneous; *KEYWORDS*: micromagnetism, transdomain, thermoremanent magnetisation, magnetic stability, magnetic structures, magnetite

Citation: Muxworthy, A. R., D. J. Dunlop, and W. Williams, High-temperature magnetic stability of small magnetite particles, *J. Geophys. Res.*, 108(B5), 2281, doi:10.1029/2002JB002195, 2003.

1. Introduction

[3] The stability of magnetic remanence over geological timescales is essential to palaeomagnetism. Only if magnetic remanence is stable over such timescales can its measured direction and intensity be meaningful to the interpretation of geological problems.

[4] The stability of a grain's magnetic remanence has long been known to depend on its size. The remanence carried by the smallest grains, i.e., magnetic single domain (SD) grains (Figure 1a), has been shown both experimen-

tally and theoretically to be very stable over long time-scales. SD theories [Néel, 1949; Walton, 1980] adequately explain the observed SD behavior [Dunlop and West, 1969; Williams and Walton, 1988]. Larger grains which are magnetically multidomain (MD), have been shown experimentally to display a very stable fraction of remanence [McClelland and Shcherbakov, 1995; Özdemir and Dunlop, 1998]. The relative size of this stable fraction increases as the grain size decreases [Dunlop and Argyle, 1991]. Consequently, small MD grains are relatively stable and are commonly referred to as pseudo-SD (PSD). In contrast classical analytical MD theory predicts that MD remanence should not be so stable [Néel, 1955], and does not accommodate grain size effects to explain PSD behavior.

[5] More successful in predicting PSD behavior has been direct numerical modeling of PSD domain structures using

¹Now at School of GeoSciences, University of Edinburgh, Edinburgh, UK.

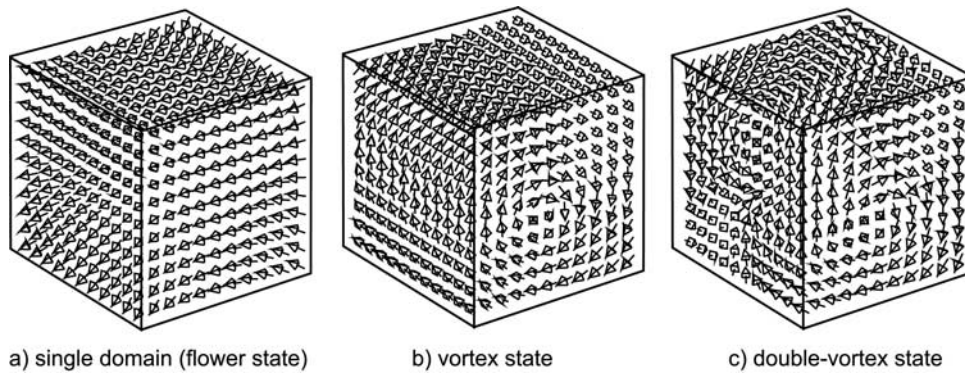


Figure 1. Domain states occurring in cubic grains of magnetite at room temperature for a grain with edge length of 120 nm (a) single domain (flower state), (b) single vortex state, and (c) double vortex state. In this paper the term “SD state” refers not just to homogeneous magnetization structures as in Néel theory but also to nonuniform domain structures as shown in Figure 1a which are basically SD-like with a degree of flowering toward the edges of the grain. The [001] axis aligns with the z axis of the cube. It was necessary to constrain Figure 1c for a 120 nm cube.

three-dimensional micromagnetic algorithms [e.g., *Williams and Dunlop*, 1989, 1995; *Fabian et al.*, 1996]. These studies have shown that the domain state of PSD grains just above the SD/MD threshold size is not a two domain structure with a 180° domain wall, as postulated by former PSD theories, but a vortex structure (Figure 1b). For slightly larger PSD grains, *Fabian et al.* [1996] have shown that a double-vortex (DV) (effectively three-domain) structure is likely (Figure 1c). In addition these models have shown that SD grains just below the SD/MD threshold display “flowering” of the domain structure near the edge of the grains (Figure 1a).

[6] In this paper we examine the stability of PSD magnetite remanence structures like those shown in Figure 1 as a function of temperature up to near the Curie temperature ($\approx 580^\circ\text{C}$) using a three-dimensional micromagnetic model with a conjugate-gradient (CG) minimization algorithm. There have been several previous papers which have examined various aspects of SD and PSD remanence stability as a function of temperature using micromagnetics [*Dunlop et al.*, 1994; *Thomson et al.*, 1994; *Winklhofer et al.*, 1997]. The results of *Dunlop et al.* [1994] were groundbreaking, but they only used a one-dimensional model. However, *Thomson et al.* [1994] and *Winklhofer et al.* [1997] both incorporated simulated annealing (SA) into their three-dimensional models which greatly increases computational time. Consequently, both studies concentrated on smaller SD/flower structures which they could accurately model, however, the larger PSD structures also considered were modeled using insufficient resolutions [*Rave et al.*, 1998]. *Winklhofer et al.* [1997] realized this and tested their SA minimizations with CG solutions determined at higher resolutions. The comparison was favorable.

[7] With the rapid improvement in computing resources it has now become feasible to model such PSD structures using the correct minimum resolution. In this paper we consider both changes in grain size (30–300 nm) and differences in shape (cubic and elongated grains up to an axial ratio q of 1.4). In addition to examining the SD-vortex transition using constrained and unconstrained models as in

previous papers, we examine for the first time the stability of DV structures (Figure 1c).

2. Discrete Micromagnetic Model

[8] The basic algorithm used to calculate the results in this paper was fully described by *Wright et al.* [1997]. The model subdivides a grain into a number of finite element subcubes. Each sub-cube represents the averaged magnetization direction of many hundreds of atomic magnetic dipole moments. All the subcubes have equal magnetic magnitude, but their magnetization can vary in direction. The domain structure was calculated by minimizing the total magnetic energy E_{tot} , which is the sum of the exchange energy E_{ex} , the magnetostatic energy E_d and the anisotropy E_{anis} [*Williams and Dunlop*, 1989; *Wright et al.*, 1997]. The domain state of a grain is calculated by minimizing E_{tot} by the CG method with a fast Fourier transform (FFT) to give the local energy minimum (LEM) [*Fabian et al.*, 1996; *Wright et al.*, 1997]. The calculation of the energy terms and the implementation of the FFT are exactly the same as in the work of *Wright et al.* [1997].

[9] It was not necessary to include magnetostrictive anisotropy in the model [*Fabian and Heider*, 1996] because for magnetite grains < 5000 nm in size, its contribution is insignificant over the temperature range considered in this paper [*Muxworthy and Williams*, 1999]. The structures in this study were calculated for stress-free samples, i.e., no dislocations and no external stress, making the contribution from the magnetoelastic anisotropy zero.

[10] In the model $E_{ex} \propto$ the exchange constant A , $E_d \propto$ the spontaneous magnetization M_s and $E_{anis} \propto$ the first cubic magnetocrystalline anisotropy K_1 . The thermal behavior of A , M_s and K_1 was taken from *Heider and Williams* [1988], *Pauthenet and Bochirol* [1951], and *Fletcher and O'Reilly* [1974], respectively.

[11] To accurately model domain structures it is necessary to have a minimum model resolution of two cells per exchange length (exchange length = $\sqrt{A/K_d}$, where $K_d = \mu_0 M_s^2/2$ and μ_0 is the permeability of free space [*Rave et al.*, 1998]). This minimum resolution was used at all times in

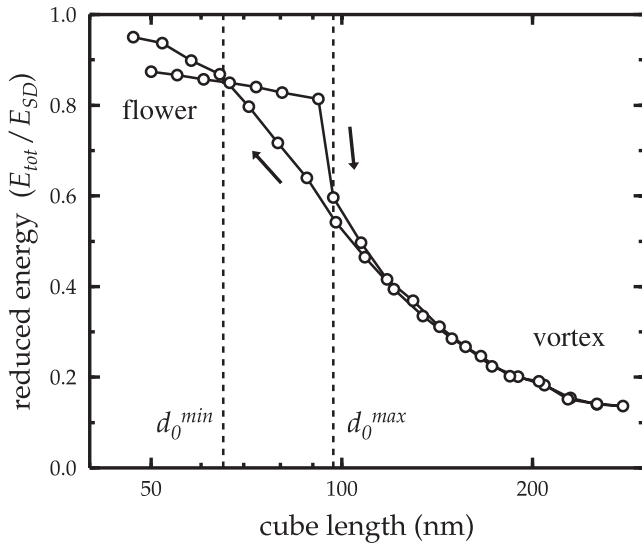


Figure 2. Energy density of a magnetite cube as a function of edge length d for an initial SD configuration at room temperature (Figure 1a). The grain size was gradually increased until the SD structure collapsed to a vortex structure at $d_0^{max} = 96$ nm. The size was then gradually decreased until a SD state formed at $d_0^{min} = 64$ nm. To maximize computer efficiency the resolution was increased/decreased with each increase/decrease in size, and the domain structure rescaled between each pair of calculations.

this study. This meant that the models were significantly larger than in previous studies, e.g., for the largest grain that *Winklhofer et al.* [1997] modeled, i.e. 120 nm, they used a resolution of $5 \times 5 \times 5$, whereas the resolution used in this study for a 120 nm grain was $17 \times 17 \times 17$.

[12] The increase in resolution meant that it was impractical to incorporate SA in the model, and the minimization was based on the CG algorithm. The SA method generally finds lower energy states than CG algorithms. However, the difference has been shown not to be significant [Thomson, 1993]. Nevertheless, the higher energy estimates from the CG algorithm are likely to lead to slightly higher energy barrier estimates between LEM states in the constrained model calculations (section 4). Therefore these results should be treated as upper energy barrier estimates.

[13] The effect of applying external fields similar to the strength of the earth's field was found to be negligible for both the constrained and unconstrained models. *Winklhofer et al.* [1997] drew similar conclusions.

3. Unconstrained Models

[14] There are several methods of determining the possible and favorable domain structure as a function of temperature. Here the unconstrained method of *Fabian et al.* [1996] and *Williams and Wright* [1998] is described. In this approach a very small grain, say ~ 20 nm, with an initial SD structure is gradually increased in size until the domain structure collapses to a vortex structure at d_0^{max} (Figure 2). The grain size is then decreased until the vortex structure becomes SD at d_0^{min} (Figure 2). d_0^{min} and d_0^{max} are inter-

preted as the lower and upper bounds where both SD and vortex structures can co-exist.

[15] Previous studies have only made these calculations at room temperature [e.g., *Fabian et al.*, 1996; *Winklhofer et al.*, 1997; *Williams and Wright*, 1998]. The room temperature curve (Figure 2) is in rough agreement with *Williams and Wright* [1998], with a transition from a SD (flower) to vortex state. In contrast, *Fabian et al.* [1996] found that the SD state collapsed to a DV structure, not a vortex state. This difference in findings raises questions about the the existence of the DV state in ideal magnetite cubes in this narrow grain size range. Clearly, for certain grain sizes, grain shapes and mineralogy, DV states will be favorable [Rave et al., 1998; *Williams and Wright*, 1998]. However, do they occur in magnetite in this grain size range? Initially, the transition from SD to DV state was thought to be due to incomplete minimization, but recent calculations suggest that it may be due to the degree of numerical precision in the model; stable DV states occur when the numerical precision of the model is high. Either the high precision calculations introduce artificial LEM states or reduced precision calculations simply “step-over” the energy barriers (K. Fabian, personal communication, 2003).

[16] d_0^{min} and d_0^{max} were determined for each temperature and are plotted as a function of temperature in Figure 3. d_0 is the average of d_0^{min} and d_0^{max} . As the temperature increases from room temperature d_0^{min} and d_0^{max} initially diverge. However, above $\sim 300^\circ\text{C}$, the stability range for SD and vortex co-existence is seen to narrow. On approach to the Curie temperature T_c , d_0^{max} increases sharply to ~ 200 nm just below T_c , and the grain size range of co-existence increases.

[17] Compared to the 1-D micromagnetic model for a grain with $q = 1.5$ [Dunlop et al., 1994], it is seen that the range where vortex states and SD states can co-exist is much narrower, especially at room temperature. From hysteresis data d_0 was estimated to be more or less inde-

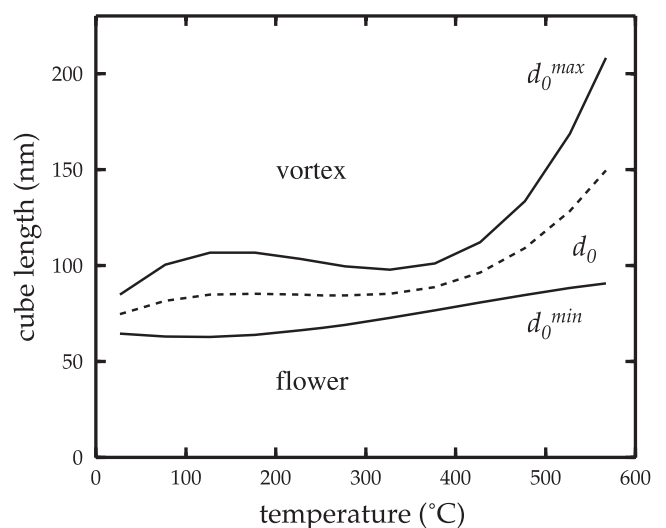


Figure 3. d_0^{max} , d_0 , and d_0^{min} versus temperature for cubic grains ($q = 1$). Above d_0^{max} only the vortex state is possible, whereas below d_0^{min} , only the flower or SD state is possible. Between d_0^{max} and d_0^{min} it is possible for the grain to be in either state.

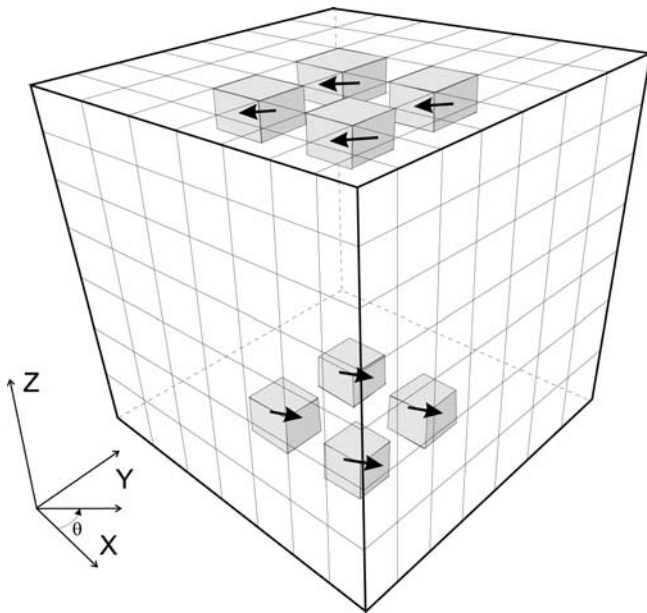


Figure 4. Schematic of the constrained SD-vortex micro-magnetic model. A number of cells at the top have their magnetization constrained to a direction θ_1 in the x - y plane, while another set of cells at the bottom are constrained to a direction θ_2 also in the x - y plane. The energy is minimized with respect to the magnetization direction of all the other cells. θ_1 and θ_2 are set to angles between 0° to 360° at interval spacings of 15° , 30° or 45° depending on model resolution. The total number of constrained cells varies with model resolution but was kept between 2 and 5% of the total.

pendent of temperature until 450°C , where it increases rapidly [Dunlop, 1987].

4. Constrained High-Temperature Models

[18] To determine the stability of an LEM state, it is necessary to calculate the energy barriers (E_B) which trap it. This is done by constraining domain structures of a grain into intermediate non-LEM states.

[19] Constrained models of domain structure were calculated using a similar procedure to that first described by Enkin and Williams [1994]. In this approach, a number of cells are constrained to set angles, and then the total energy is minimized with respect to the other unconstrained cells. This technique allows non-LEM magnetic states to be produced so that transition paths between LEM states can be examined. Two sets of constrained cells at opposite sides of the model grain are rotated through 360° at some step interval (Figure 4). From these two degrees of freedom energy surfaces can be plotted, from which the energy barriers between LEM states are determined [Enkin and Williams, 1994].

[20] Previous constrained models have only considered SD-vortex transitions [Enkin and Williams, 1994; Winklhofer et al., 1997; Muxworthy and Williams, 1999]. In this paper we also consider SD-DV and vortex-DV transitions.

[21] For very small grains near d_0 in size, considering only SD-vortex transitions is reasonable because as a first approximation there are only two LEM domain states, the

SD state and the vortex state. In fact, just as SD state have different degrees of flowering, there are different types of vortex state, e.g., Rave et al. [1998] found seven different vortex states in uniaxial materials. However, in this study we group all these vortex states into one category, as we consider the study of subtle differences between vortex states in magnetite outside the scope of this paper.

[22] As the grain size becomes larger the number of possible LEM states increases. The next most realistic LEM domain state to constrain in grains larger than d_0^{max} is the DV state (Figure 1c). To produce DV structures it is necessary to constrain the edges of the models, not the surfaces as in SD-vortex constrained models (Figure 4), i.e., the four corners of the middle layer of cells lying in the z plane were constrained. To obtain SD-DV transitions, the constrained cells in the four corner groups were split into two pairs facing each other across the diagonal. Each pair was then rotated separately through 180° . To produce DV-vortex transition paths, two sets of constrained cells separated by the edge of the cube were kept fixed and were anti-parallel, while the other two sets were rotated independently through 180° . As the number of possible LEM states becomes greater, the number of possible transition paths between LEM states increases. It is possible therefore that in constraining SD-DV and DV-vortex transitions, some transition paths with lower energy barriers are overlooked, e.g., an SD to DV transition with an intermediate vortex state. Therefore the energy barriers determined for DV-SD and DV-vortex transitions could possibly be overestimates. This problem is not unique to constrained CG minimizations, but also applies to constrained SA calculations.

[23] Energy-surface plots were determined as a function of grain size, temperature and shape (Figure 5). As the grain size increased, the model resolution was increased, e.g., for a 100 nm cubic grain the resolution was $14 \times 14 \times 14$ and for a 300 nm grain the resolution was $44 \times 44 \times 44$. As the larger grain sizes required more CPU time, less variation in temperature and shape could be examined for these grains. Elongated grains were considered as cuboids of square cross-section and elongated along one axis. This meant that the model size had to be increased, e.g., for the 300 nm model with a long axis/short axis ratio $q = 1.4$, the grid size was $62 \times 44 \times 44$. The number of constrained cells increased with resolution but was kept to ~ 2 –5% of the total number of cells. During the energy-surface plot calculations, domain structures were visually checked for smooth consistent behavior with no abrupt changes.

[24] The minimum energy barrier between LEM states was determined by considering saddle-points between metastable states (Figure 5). In particular, transition paths from vortex and DV states were difficult to determine. In these cases, the energy barrier was defined as the energy needed to rotate the moment by 90° .

4.1. SD-Vortex Transitions

[25] For the SD-vortex transition, two sets of spins were constrained on opposite sides of the grain in an identical procedure to that of Enkin and Williams [1994]. Typical energy-surface plots are shown in Figure 6 for a grain with $d = 120$ nm and $q = 1.2$. At room temperature the vortex state is the most favorable LEM state (Figure 6a). The energy barrier (E_B) between two such identical states was

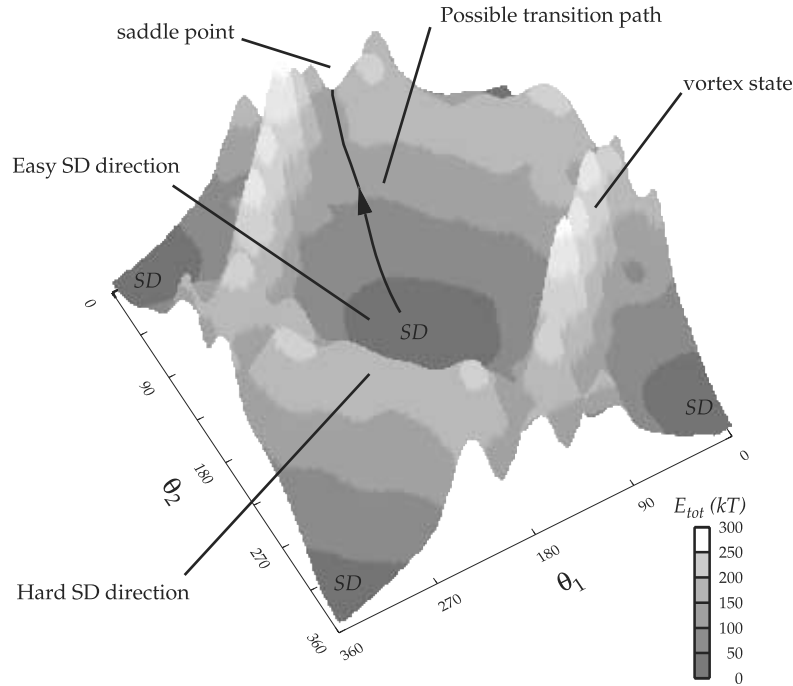


Figure 5. SD-vortex energy surface (contour map of $(E_{tot} - \text{minimum } E_{tot})/kT$ for different constrained three-dimensional magnetic structures) for a grain with edge 120 nm and $q = 1.4$ at 567°C . As the grain is asymmetric, there are favorable (easy) and unfavorable (hard) SD magnetic states. Unfavorable vortex structures are also marked. A possible transition path over a saddle point is highlighted. The two angles θ_1 and θ_2 refer to the angles of the two sets of constrained spins (Figure 4). The model resolution used was $24 \times 17 \times 17$.

determined to be 590 kT. At 567°C the SD state is the most favorable LEM state and the energy barrier between two identical SD states was calculated to be 6.1 kT.

[26] From such energy plots, energy barriers (E_B) were determined as a function of temperature (Figure 7). Included on Figure 7 are the Boltzmann energies for two relaxation times; a laboratory relaxation time ~ 1 s giving $E_B \approx 25$ kT and a geological relaxation time ~ 1 billion yrs with $E_B \approx 60$ kT. At high temperatures near T_c , $E_B < 25kT$ for all grain sizes and shapes. However, as the temperature decreases, E_B increases sharply. The rate of increase is greatest for larger grains, and at room temperature the largest grain (300 nm) has the largest E_B . It is at first sight surprising that grains with SD states have lower energy barriers than grains with vortex states. However, this is due to a combination of effects.

[27] Firstly the competing magnetic energies increase with grain volume. For example, in a first approximation for simple magnetic structures, E_{ex} and E_{anis} increase linearly with grain volume, while the magnetostatic energy E_d increases as the square of grain volume. The magnetostatic energy's strong grain size dependence causes both E_{tot} and E_B to increase sharply with grain size.

[28] Secondly the configurational anisotropy displays a grain size dependency. The configurational anisotropy is a term coined to describe the energy barrier associated with intermediate states in a transition path. Temporarily ignoring magnetocrystalline anisotropy, consider a SD-like or flower state in a cubic grain (Figure 1a). The energy of a SD state aligned along "x" or "y" are equivalent due to symmetry;

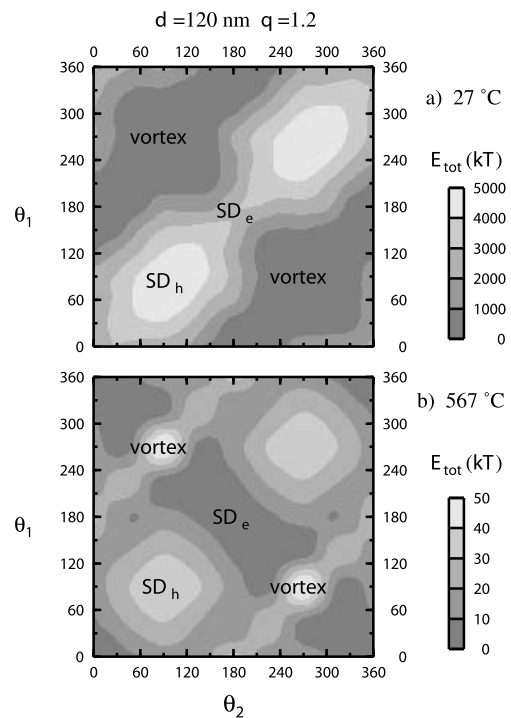


Figure 6. SD-vortex energy surfaces for a grain with edge 120 nm and $q = 1.2$ at (a) room temperature and (b) just below T_c . As the grain is asymmetric there are hard (SD_h) and easy (SD_e) magnetic directions. Favorable vortex structures are also marked. The model resolution used was $21 \times 17 \times 17$.

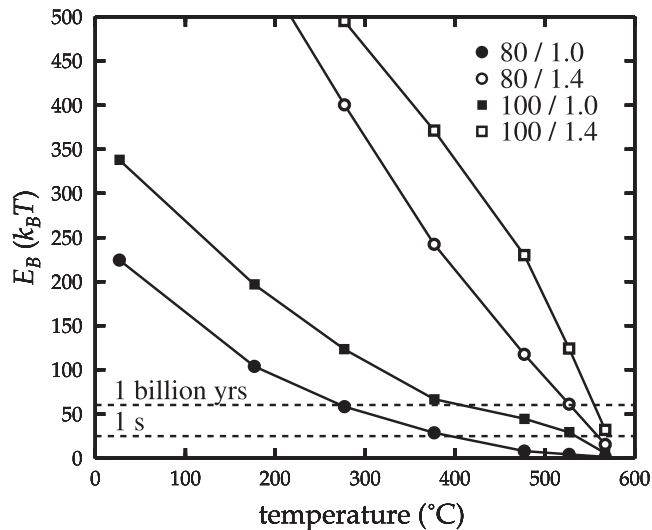


Figure 7. Energy barrier (E_B) as a function of temperature for a selection of small particles of magnetite; two with $d = 80$ nm ($q = 1$ and 1.4) and two for $d = 100$ nm ($q = 1$ and 1.4). The two dashed lines at $E_B = 60$ kT and 25 kT represent the palaeomagnetic and laboratory stability criteria.

the degree of flowering will be identical. For a SD to rotate coherently from the x direction to the y direction or vice versa it will have to pass through an intermediate state. The degree of flowering varies depending on the direction of the magnetization with respect to the cube faces. Intermediate states have less flowering due to geometry considerations giving rise to an effective energy barrier. If no flowering occurs, i.e., an ideal SD grain, then for cubic grains with no magnetocrystalline anisotropy there would be no energy barrier for this rotation. However, in magnetite flowering is in reality common. Since the degree of flowering increases as the grain size increases, the energy barrier along the transition path increases. This effect occurs for other types of transitions, e.g., between vortex states. Configurational

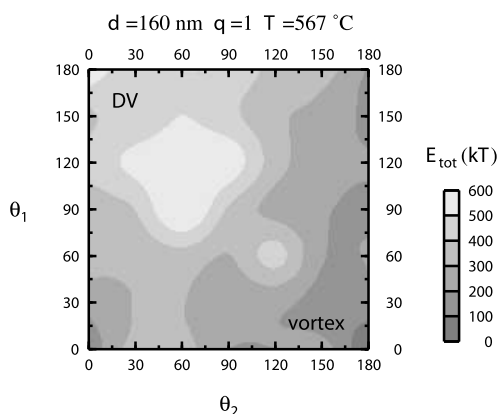


Figure 8. DV-vortex energy surface for a grain with edge 160 nm and $q = 1.0$ just below T_c . The regions for DV structures and vortex structures are highlighted. Intermediate structures are positioned in between these two domain states. The model resolution used was $23 \times 23 \times 23$. θ_1 and θ_2 refer to the angles of the two sets of constrained spins, see text for explanation.

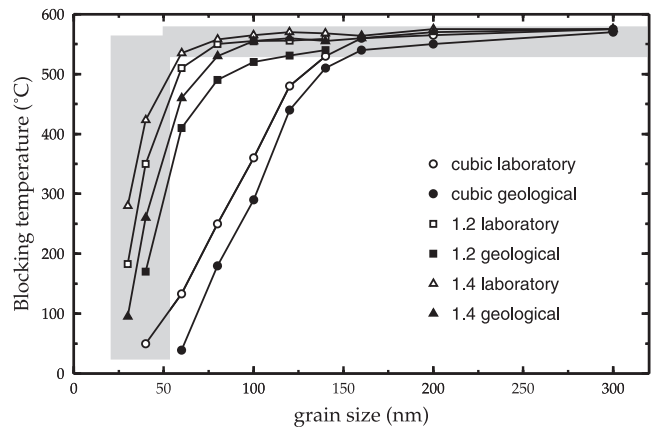


Figure 9. Calculated blocking temperatures as a function of grain size for different aspect ratios ($q = 1$ (cubic), 1.2 and 1.4). Open symbols represent blocking temperatures in cooling under laboratory conditions, while solid symbols indicate cooling over geological timescales. The shaded areas represent experimentally obtained blocking temperatures from three magnetite samples of near cubic shape [Dunlop, 1973].

anisotropy will always exist in cubic structures, but will often be masked by magnetocrystalline anisotropy or other anisotropy created by applied fields. Only a sphere will have no configurational anisotropy.

[29] Generally, the results agree well with those of Winklhofer *et al.* [1997] who modeled grains up to 120 nm using simulated annealing. The agreement is good even for the larger grains where Winklhofer *et al.* [1997] used a resolution of only $5 \times 5 \times 5$.

4.2. SD-DV and Vortex-DV Transitions

[30] SD-DV and vortex-DV transitions were determined for grains in the range 140 – 200 nm. Below 140 nm, the DV state is not an LEM state [Fabian *et al.*, 1996]. Both SD and DV states were found to be LEM states in this size range and produced energy surface plots similar to those in Figure 6. The DV-vortex energy surfaces are less easily interpreted (Figure 8). Generally the vortex state was the absolute energy minimum, and the DV state had a much higher energy. The DV state was often located near very shallow LEM states, which are not thought to be stable (the model does not include thermal fluctuations which would make them even less stable). This implies that even if the grain is in a stable LEM state in a SD-DV energy plot diagram, in an unconstrained system the DV state would actually minimize to a vortex state, in effect resulting in a SD-vortex energy surface plot (Figures 5 and 6). Because the DV state was not a significant LEM state, no values for E_B were determined.

5. Blocking Temperatures and Relaxation Times

[31] From plots of E_B versus temperature (Figure 7), blocking temperature diagrams as a function of grain size were determined (Figure 9). Also shown in Figure 9 are the experimental data of Dunlop [1973]. As the grain size increases, the blocking temperature increases, reflecting the increase in E_B with grain size (Figure 7). As q increases

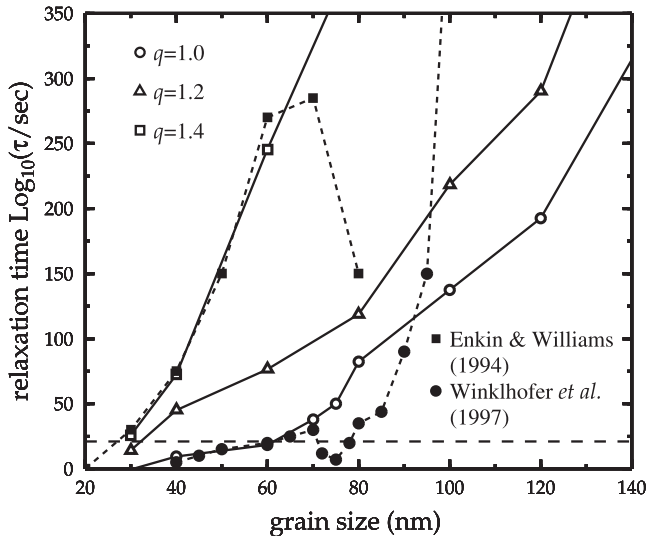


Figure 10. Logarithm of relaxation time τ versus edge length d for $q = 1$ (cubic), 1.2 and 1.4 magnetites at room temperature as a function of grain size. The dashed horizontal line corresponds to $\tau = 1$ Ma. The results of [Enkin and Williams, 1994] and [Winklhofer et al., 1997] for cubic grains are also shown.

the blocking temperature increases. The effect of blocking time, i.e., geological (1 billion years, $E_B < 60$ kT) versus laboratory (1 s, $E_B < 25$ kT), is seen to be relatively small compared to changes in grain geometry. Figure 9 is similar to Figure 7 of Winklhofer et al. [1997], though they did not calculate blocking temperatures for grains greater than 120 nm. Our model results agree well with the experimental data of Dunlop [1973]. That the blocking temperature continues to increase as the grain size is increased above d_0 implies that small PSD grains up to 300 nm in size are magnetically more stable than SD grains. This goes against traditional Néel-type models [Néel, 1949, 1955] for SD and MD behavior, but importantly agrees with the experimental results of Dunlop [1973]. The high-stability of micromagnetic PSD structures is associated with the increase in E_B with grain size discussed above.

[32] In addition to determining blocking temperature curves, it is possible to approximate the logarithmic relaxation time as a function of grain size at room temperature (Figure 10). This is only an approximation as it is based on Néel's theory for coherent rotation of SD uniaxial grains [Néel, 1949]. Figure 10 depicts the amount of time it would take for an assemblage of such grains to unblock at room temperature, i.e., it is a measure of magnetic viscosity. Similar calculations have been made by Enkin and Williams [1994] and Winklhofer et al. [1997] for cubic grains, and their results are depicted in Figure 10. As q is increased, the relaxation time is observed to increase, that is, the magnetic moment becomes less viscous. There is a clear jump in behavior between $q = 1.2$ and 1.4.

[33] The results for the cubic grains ($q = 1$) in this paper are closer to the results of [Winklhofer et al., 1997] than to the results of Enkin and Williams [1994]. The $q = 1$ curve follows the data of Winklhofer et al. [1997] closely until ~ 70 nm. Above this size, the $q = 1$ data in this paper

continue to increase steadily, whereas the data of Winklhofer et al. [1997] decrease around 75 nm before increasing sharply at $d = 90$ nm. It is suggested that this divergence between results may be due to differences in the micro-magnetic model resolutions which similarly diverge as the grain size is increased. Alternatively, the SA algorithm of Winklhofer et al. [1997] may have found a lower energy state than the CG algorithm in this paper.

[34] In addition there are differences in crystal symmetry; in this paper the [001] axis is aligned with the z axis and the model is symmetrical with respect to the three axis, whereas the model of Winklhofer et al. [1997] had [111] aligned with the z axis, i.e., only one easy axis was aligned along a crystal axis edge. As the preference for the domain structure is to align with the cube edges, the shape contribution and cubic anisotropy combine effectively to form a uniaxial anisotropy aligned in the z -direction. This difference in symmetry may have some effect. Winklhofer et al. [1997] attribute their model behavior at around 75 nm to the switch from uniform to nonuniform reversal processes.

6. Transdomain Thermoremanence

[35] In the previous sections, the magnetic stability was determined by considering the energy barrier between LEM states at each temperature regardless of domain state type. Transdomain thermoremanence (TRM) analysis, in contrast, looks at possible transitions between different types of LEM states, e.g., SD to vortex, as the temperature changes [Moon and Merrill, 1986; Dunlop et al., 1994]. It focuses on domain states where energy barriers between LEM states are $< 25kT$, for laboratory observational timescales, and uses Boltzmann statistics to determine equilibrium probabilities for competing LEM states. From this type of analysis it is possible to predict the behavior of a remanence during heating and cooling.

[36] When $E_B < 25kT$ between two possible LEM states, thermal excitations between the states occur frequently. In this thermal equilibrium or superparamagnetic condition of rapid transitions between the states, neither LEM state is stable for long enough to preserve a remanence, but the LEM state with the lower energy is more probable or frequently occupied. The equilibrium Boltzmann probability of each state is

$$p_{eq}^i = Z^{-1} \exp(-E_i/kT) \quad (1)$$

where Z is the partition function or sum of exponential factors over all states.

[37] On examination of all the temperature sequences of energy plots in this study, transdomain TRM effects were only found to occur in a small number of sequences, e.g., for $d = 80$ nm and $q = 1.0$, and $d = 100$ nm and $q = 1.2$. Only SD-vortex transdomain transitions were observed. No transdomain transitions were found which involved DV states.

[38] The grain size and shape which displayed the best example of transdomain TRM was for $d = 80$ nm and $q = 1.0$. This grain size was studied in detail in and near the transdomain transition temperature range (Figure 11). It was found that between 417°C and 422°C , there is a

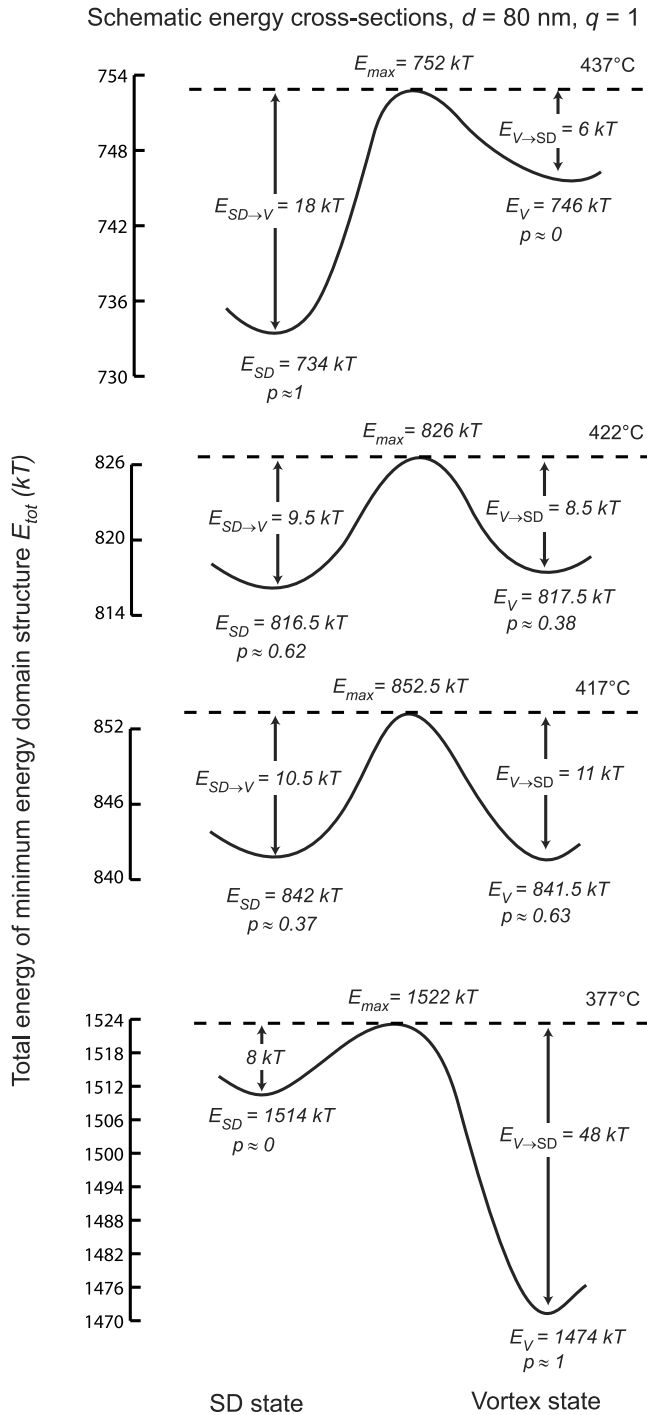


Figure 11. Schematic of high-temperature energy barriers for SD \leftrightarrow Vortex (V) transitions in a $d = 80$ nm and $q = 1$ magnetite grain. Proceeding from top to bottom simulates cooling (TRM acquisition in the presence of a small field), whereas from bottom to top simulates thermal demagnetization. The Boltzmann probabilities calculated from equation (1) for each state are also shown. The energy scale on the upper three diagrams is identical.

transdomain process with the vortex state being more favorable at 417°C and the SD state at 422°C . The energy barriers in this temperature range are less than $25kT$. Therefore domains will not become trapped in an

unfavorable state on cooling or warming through this temperature.

[39] If a cubic grain with size 80 nm is cooled from T_c to room temperature, it would initially lie in the SD state which is by far the most probable state ($p \approx 1$) on cooling from T_c to 437°C (the first schematic in the series), though it should be noted that at all times $E_{SD \rightarrow V} < 25 kT$ and $E_{V \rightarrow SD} < 25 kT$. On cooling to 422°C , the SD state ($p = 0.62$) and vortex state ($p = 0.38$) have very similar energies, although the SD state is still slightly more favorable. However, the change in equilibrium states, e.g., $p = 0.62$ for the SD state compared to $p \approx 1$ at 437°C , means that any TRM carried by an assemblage of such grains will be reduced. On cooling to 417°C , the roles have been reversed as the vortex state is now the slightly more favorable state. On cooling further to 377°C , the vortex state is now decisively the equilibrium state ($p \approx 1$) and is effectively blocked, i.e., on a laboratory timescale it is not possible for a vortex state to jump to a SD state. On cooling to room temperature, $E_{V \rightarrow SD}$ continues to increase while $E_{SD \rightarrow V}$ remains $\leq 25 kT$.

[40] Dunlop *et al.* [1994] investigated transdomain TRM using a constrained one-dimensional micromagnetic model, from which they were able to determine the probabilities of transdomain TRM occurring between SD, two- and three-domain states. They found in contrast to Figure 11 that all transdomain processes occurred above 553°C . The difference between the two results is attributed to the models. It is widely acknowledged that increasing the number of dimensions in micromagnetic models decreases the absolute energy barriers.

7. Discussion and Conclusion

[41] The energy barriers associated with larger grains in vortex states are significantly higher than those of smaller grains in SD states. This implies that small PSD grains have in fact higher stability of remanence than SD grains, and in addition that the grain size range which provides reliable and meaningful magnetic signals is greater than previously predicted. The reason for the high-stability of PSD grains is due to relative increases with grain size of both the magnetostatic energy and the configurational anisotropy. However, it should be noted, that as the grain size increases it is likely that E_B is increasingly over-estimated, because we have only considered a few constrained transition paths. As the grain size becomes larger the number of possible transition paths increases. It becomes impractical to determine all these paths, and hence it is possible that some lower energy transitions have not been determined. A possible way forward is to use simulated annealing techniques to examine many more possible transition paths, but these methods have yet to be fully exploited in micromagnetism.

[42] The grain sizes which display the highest stability of remanence are larger than those found by other stability criteria, in particular those determined from hysteresis measurements, e.g., the coercive force. Generally, from hysteresis measurements and the interpretation of them, SD grains are considered to be magnetically more stable than PSD or larger MD grains, i.e., in a magnetic field SD grains are more stable than PSD grains. In contrast, the findings in this study show that the time/temperature stabil-

ity of PSD remanence is greater than that of SD remanence, i.e., in a zero field PSD grains are more stable than SD grains. The reason for this difference is thought to be due to the different systems which we are examining. In the presence of an external field, it appears that larger PSD-size grains can more readily change their structure to accommodate the external field energy than SD grains. However, in zero field the larger PSD grains have larger energy barriers to overcome due to the increase in the magnetostatic energy and configurational anisotropy associated with their larger grain size.

[43] Transdomain TRM analysis of small PSD grains indicates that there are a limited number of grain sizes and shapes which will nucleate domain wall-type structures during cooling (Figure 11). Such nucleation events would cause the total measured remanence to decrease with cooling, in conflict with the theories of Néel [1949, 1955] for remanence cooling behavior. However, decreases in remanence on cooling in zero field have been widely reported [e.g., McClelland and Sugiura, 1987; Muxworthy, 2000]. In addition, direct high-temperature domain observations on large low-stress MD grains produced by hydrothermal recrystallization found that domain walls in larger MD grains moved readily and nucleation was common in small fields [Heider et al., 1988]. This contradiction between Néel's theories and experimental measurements has long been a problem in TRM acquisition theories. This is the first time that a theoretical model has come close to providing a direct physical explanation for this effect. In this paper we have considered only small PSD grains. However, on comparison with the experimental data, it can be inferred that similar processes are occurring in larger MD grains. The fact that it occurs at relatively low temperatures is also in agreement with magnetic measurements and domain observations. Attempts were made to simulate nucleation effects during cooling, but without thermal agitation the model failed to nucleate the vortex structure as predicted by energy-surface plots.

[44] The DV state, which was found to be a LEM state in the studies of Fabian et al. [1996], was found to be either not a LEM state or only a very shallow one, suggesting that for the grain sizes considered in this study, DV structures are unlikely to occur in unconstrained simulation models.

[45] **Acknowledgments.** We enjoyed stimulating discussions with Claire Carvallo, and we would like to thank the late Kenneth McLean for computing support. This paper benefited from the comments of Karl Fabian and an anonymous reviewer. This research supported by the Natural Sciences and Engineering Research Council of Canada through grant A7709 to D.J.D.

References

- Dunlop, D. J., Thermoremanent magnetization in submicroscopic magnetite, *J. Geophys. Res.*, **78**, 7602–7613, 1973.
- Dunlop, D. J., Temperature dependence of hysteresis in 0.04–0.22 μm magnetites and implications for domain structure, *Phys. Earth Planet. Inter.*, **46**, 100–119, 1987.
- Dunlop, D. J., and K. S. Argyle, Separating multidomain and single-domain-like remanences in pseudo-single-domain magnetites (215–540 nm) by low-temperature demagnetisation, *J. Geophys. Res.*, **96**, 2007–2017, 1991.
- Dunlop, D. J., and G. F. West, An experimental evaluation of single domain theories, *Rev. Geophys.*, **7**, 709–757, 1969.
- Dunlop, D. J., A. J. Newell, and R. J. Enkin, Transdomain thermoremanent magnetization, *J. Geophys. Res.*, **99**, 19,741–19,755, 1994.
- Enkin, R. J., and W. Williams, Three-dimensional micromagnetic analysis of stability in fine magnetic grains, *J. Geophys. Res.*, **99**, 611–618, 1994.
- Fabian, K., and F. Heider, How to include magnetostriction in micromagnetic models of titanomagnetite grains, *Geophys. Res. Lett.*, **23**, 2839–2842, 1996.
- Fabian, K., A. Kirchner, W. Williams, F. Heider, T. Leibl, and A. Hubert, Three-dimensional micromagnetic calculations for magnetite using FFT, *Geophys. J. Int.*, **124**, 89–104, 1996.
- Fletcher, E. J., and W. O'Reilly, Contribution of Fe^{2+} ions to the magnetocrystalline anisotropy constant K_1 of $\text{Fe}_{3-x}\text{Ti}_x\text{O}_4$ ($0 < x < 0.1$), *J. Phys. C. Solid State Phys.*, **7**, 171–178, 1974.
- Heider, F., and W. Williams, Note on temperature dependence of exchange constant in magnetite, *Geophys. Res. Lett.*, **15**, 184–187, 1988.
- Heider, F., S. L. Halgedahl, and D. J. Dunlop, Temperature dependence of magnetic domains in magnetite crystals, *Geophys. Res. Lett.*, **15**, 499–502, 1988.
- McClelland, E., and V. P. Shcherbakov, Metastability of domain state in MD magnetite: Consequences for remanence acquisition, *J. Geophys. Res.*, **100**, 3841–3857, 1995.
- McClelland, E., and N. Sugiura, A kinematic model of TRM acquisition in multidomain magnetite, *Earth Planet. Sci. Lett.*, **46**, 9–23, 1987.
- Moon, T., and R. T. Merrill, A new mechanism for stable viscous remanent magnetization and overprinting during long magnetic polarity intervals, *Geophys. Res. Lett.*, **13**, 737–740, 1986.
- Muxworthy, A. R., Cooling behaviour of partial thermoremanences induced in multidomain magnetite, *Earth Planet. Sci. Lett.*, **184**, 149–159, 2000.
- Muxworthy, A. R., and W. Williams, Micromagnetic models of pseudo-single domain grains of magnetite near the Verwey transition, *J. Geophys. Res.*, **104**, 29,203–29,218, 1999.
- Néel, L., Théorie du trainage magnétique des ferromagnétiques en grains fins avec applications aux terres cuites, *Ann. Géophys.*, **5**, 99–136, 1949.
- Néel, L., Some theoretical aspects of rock magnetism, *Adv. Phys.*, **4**, 191–242, 1955.
- Özdemir, Ö., and D. J. Dunlop, Single-domain-like behavior in a 3-mm natural single crystal of magnetite, *J. Geophys. Res.*, **103**, 2549–2562, 1998.
- Pauthenet, R., and L. Bochirol, Aimantation spontanée des ferrites, *J. Phys. Radium*, **12**, 249–251, 1951.
- Rave, W., K. Fabian, and A. Hubert, The magnetic states of small cubic magnetic particles with uniaxial anisotropy, *J. Magn. Magn. Mater.*, **190**, 332–348, 1998.
- Thomson, L. C., A three-dimensional micromagnetic investigation of the magnetic properties and structures of magnetite, Ph.D. thesis, Univ. of Edinburgh, Edinburgh, UK, 1993.
- Thomson, L. C., R. J. Enkin, and W. Williams, Simulated annealing of three dimensional micromagnetic structures and simulated thermoremanent magnetization, *J. Geophys. Res.*, **99**, 603–606, 1994.
- Walton, D., Time-temperature relations in the magnetisation of assemblies of single domain grains, *Nature*, **286**, 245–247, 1980.
- Williams, W., and D. J. Dunlop, Three-dimensional micromagnetic modelling of ferromagnetic domain structure, *Nature*, **377**, 634–637, 1989.
- Williams, W., and D. J. Dunlop, Simulation of magnetic hysteresis in pseudo-single-domain grains of magnetite, *J. Geophys. Res.*, **100**, 3859–3871, 1995.
- Williams, W., and D. Walton, Thermal cleaning of viscous magnetic moments, *Geophys. Res. Lett.*, **15**, 1089–1092, 1988.
- Williams, W., and T. M. Wright, High resolution micromagnetic models of fine grains of magnetite, *J. Geophys. Res.*, **103**, 30,537–30,550, 1998.
- Winklhofer, M., K. Fabian, and F. Heider, Magnetic blocking temperature of magnetite calculated with a three-dimensional micromagnetic model, *J. Geophys. Res.*, **102**, 22,695–22,709, 1997.
- Wright, T., M. Williams, and W. Dunlop, An improved algorithm for micromagnetics, *J. Geophys. Res.*, **102**, 12,085–12,094, 1997.

D. J. Dunlop, Department of Physics, University of Toronto at Mississauga, Mississauga, Ontario, Canada L5L 1C6. (dunlop@physics.utoronto.ca)

A. R. Muxworthy and W. Williams, Grant Institute, School of GeoSciences, University of Edinburgh, West Mains Road, Edinburgh, EH9 3JW, UK. (adrian.muxworthy@ed.ac.uk)